

Comparative study of the scalar- and tensor-meson production in the reaction $\gamma\gamma^*(Q^2) \rightarrow \eta\pi^0$

N.N. Achasov^a, A.V. Kiselev^{a,b}, and G.N. Shestakov^a

^a*Laboratory of Theoretical Physics, Sobolev Institute
for Mathematics, 630090, Novosibirsk, Russia*

^b*Novosibirsk State University, 630090, Novosibirsk, Russia*

(Dated: August 23, 2016)

Abstract

The prediction of the cross section $\sigma(\gamma\gamma^*(Q^2) \rightarrow \eta\pi^0)$ based on the simultaneous description of the Belle data on the $\gamma\gamma \rightarrow \eta\pi^0$ reaction and the KLOE data on the $\phi \rightarrow \eta\pi^0\gamma$ decay is presented. The production of the scalar $a_0(980)$ and tensor $a_2(1320)$ is studied in detail. It is shown that the QCD based asymptotics of the $\gamma^*(Q^2)\gamma \rightarrow a_2(1320) \rightarrow \eta\pi^0$ cross section can be reached by the compensation of the contributions of $\rho(770)$ and $\omega(782)$ with the contributions of their radial excitations in Q^2 channel. At large Q^2 the $a_2(1320)$ contribution is expected to be dominant, while at $Q^2 = 0$ it is similar to the scalars contribution.

PACS numbers: 12.39.-x 13.40.Hq 13.66.Bc

I. INTRODUCTION

Study of the nature of light scalars $a_0(980)$ and $f_0(980)$, well-established part of the proposed light scalar meson nonet [1], is one of the central problems of nonperturbative QCD, it is important for understanding the way chiral symmetry is realized in the low energy region and, consequently, for the understanding of confinement. Many papers have already been devoted to this subject, see, for example, Refs. [2–9].

Naively one could think that the scalar $a_0(980)$ and $f_0(980)$ mesons are the $q\bar{q}$ P-wave states with the same quark structure as $a_2(1320)$ and $f_2(1270)$, respectively. But now there are many indications that the above scalars are four-quark states, see, for example, Refs. [10–25] and references therein.

One of these indications is the suppression of the $a_0(980)$ and $f_0(980)$ resonances in the $\gamma\gamma \rightarrow \eta\pi^0$ and $\gamma\gamma \rightarrow \pi\pi$ reactions, respectively, predicted in 1982 [13] and confirmed by experiment [1], see [26]. The elucidation of the mechanisms of the $\sigma(600)$, $f_0(980)$, and $a_0(980)$ resonance production in the $\gamma\gamma$ collisions confirmed their four-quark structure [14, 23–25]. Light scalar mesons are produced in $\gamma\gamma$ collisions mainly via rescatterings, that is, via the four-quark transitions. As for the $a_2(1320)$ and $f_2(1270)$, the well-known $q\bar{q}$ states, they are produced mainly via the two quark transitions (direct couplings with $\gamma\gamma$).

Another argument in favor of the four-quark nature of the $a_0(980)$ and $f_0(980)$ is the fact that the $\phi(1020) \rightarrow a_0\gamma$ and $\phi(1020) \rightarrow f_0\gamma$ decays proceed through the kaon loop: $\phi \rightarrow K^+K^- \rightarrow a_0\gamma$, $\phi \rightarrow K^+K^- \rightarrow f_0\gamma$, i.e. via the four-quark transition [15, 16, 19, 21, 22]. The kaon loop model was suggested in Ref. [15] and confirmed by the experiment ten years later [17, 18, 20].

Recently the comparative study of the scalar and tensor mesons was proposed in the $e^+e^- \rightarrow \gamma^* \rightarrow (a_0 + a_2)\gamma \rightarrow \eta\pi^0\gamma$ and $e^+e^- \rightarrow \gamma^* \rightarrow (f_0 + f_2)\gamma \rightarrow \pi^0\pi^0\gamma$ reactions (i.e. in the timelike region of γ^*) [27].

In the present study we consider the reaction $\gamma^*\gamma \rightarrow \pi^0\eta$ in the spacelike region of γ^* .

In 2009 Belle Collaboration published high-statistical data on the $\gamma\gamma \rightarrow \eta\pi^0$ reaction [28]. These data revealed the specific feature of the $\gamma\gamma \rightarrow \pi^0\eta$ cross section: it turned out sizable in the region between the $a_0(980)$ and $a_2(1320)$ resonances, that certainly indicates the presence of additional contributions. The experimenters took into account the putative heavy isovector scalar a'_0 with mass about 1.3 GeV (they called it $a(Y)$) along with $a_0(980)$

and $a_2(1320)$ together with the polynomial coherent background [28].

In the theoretical works Refs. [24, 25] $a_0(980)$ is produced mainly by loops, and the Born contribution to $\gamma\gamma \rightarrow \eta\pi^0$ plays role of coherent background, see Figs. 1, 2. The kaon formfactor $G_{K^+}(t, u)$ in loop diagrams $\gamma\gamma \rightarrow K^+K^- \rightarrow a_0$ was introduced in those papers.

The given paper is the development of the Refs. [24, 25]. Basing on their theoretical results, we perform new fitting of the Belle data simultaneously with the KLOE data on the $\phi \rightarrow \eta\pi^0\gamma$ decay. We show that in the kaon loop model of the $\gamma\gamma \rightarrow K^+K^- \rightarrow a_0$ transition the kaon formfactor $G_{K^+}(t, u)$ is not required for good data description, as well as in the $\phi \rightarrow K^+K^- \rightarrow a_0\gamma \rightarrow \eta\pi^0\gamma$ decay and $\phi \rightarrow K^+K^- \rightarrow f_0\gamma \rightarrow \pi^0\pi^0\gamma$ [15–22]. The obtained $a_0(980)$ coupling constants are in good agreement with the four-quark model prediction [15].

Using results on $\gamma\gamma \rightarrow \eta\pi^0$ we predict the $\sigma(\gamma^*(Q^2)\gamma \rightarrow \eta\pi^0, s)$, where s is the $\gamma^*\gamma$ invariant mass and Q^2 is the γ^* virtuality.

The measurement of the cross section $\sigma(\gamma^*(Q^2)\gamma \rightarrow \eta\pi^0, s)$ would allow additional check of the models of the $a_0(980)$ structure and our understanding of the mechanism of the reactions $\gamma^*\gamma \rightarrow \eta\pi^0$ as well as $\gamma\gamma \rightarrow \eta\pi^0$.

The theoretical description of the $\gamma^*\gamma \rightarrow \eta\pi^0$ reaction is in Sec. II. The results on the $\gamma\gamma \rightarrow \eta\pi^0$ data description are presented in Sec. III. The prediction of the $\sigma(\gamma^*(Q^2)\gamma \rightarrow \eta\pi^0, s)$ is in Sec. IV. It is found that the role of vector excitations (ρ' , ω' , etc.) is crucial for the $a_2(1320)$ and $f_2(1270)$ production: the QCD based asymptotics of the $\gamma^*(Q^2)\gamma \rightarrow a_2(1320) \rightarrow \eta\pi^0$ (or $\gamma^*(Q^2)\gamma \rightarrow f_2(1270) \rightarrow \pi^0\pi^0$) cross section can be reached only by taking into account cancellation of the contributions of $\rho(770)$, $\omega(782)$ and $\phi(1020)$ in Q^2 channel with the contributions of their radial excitations. The $a_2(1320)$ contribution is expected to be dominant at large Q^2 , while at $Q^2 = 0$ it is similar to the $a_0(980) + a'_0$ contribution. The conclusion is in Sec. V. Some details are provided in Appendices I–III.

Noticed misprints of Refs. [24, 25] are mentioned in Ref. [29].

II. THEORETICAL DESCRIPTION OF THE $\gamma^*\gamma \rightarrow \eta\pi^0$ REACTION

All formulas for the $\gamma\gamma \rightarrow \eta\pi^0$ reaction were derived in Refs. [24, 25], these results are used to fit the experimental data. In this section we derive formulas for the $\gamma^*(q)\gamma(k) \rightarrow \eta(q_1)\pi^0(q_2)$ reaction, $Q^2 = -q^2 > 0$. The results of Refs. [24, 25] are reached in the limit $Q^2 \rightarrow 0$.

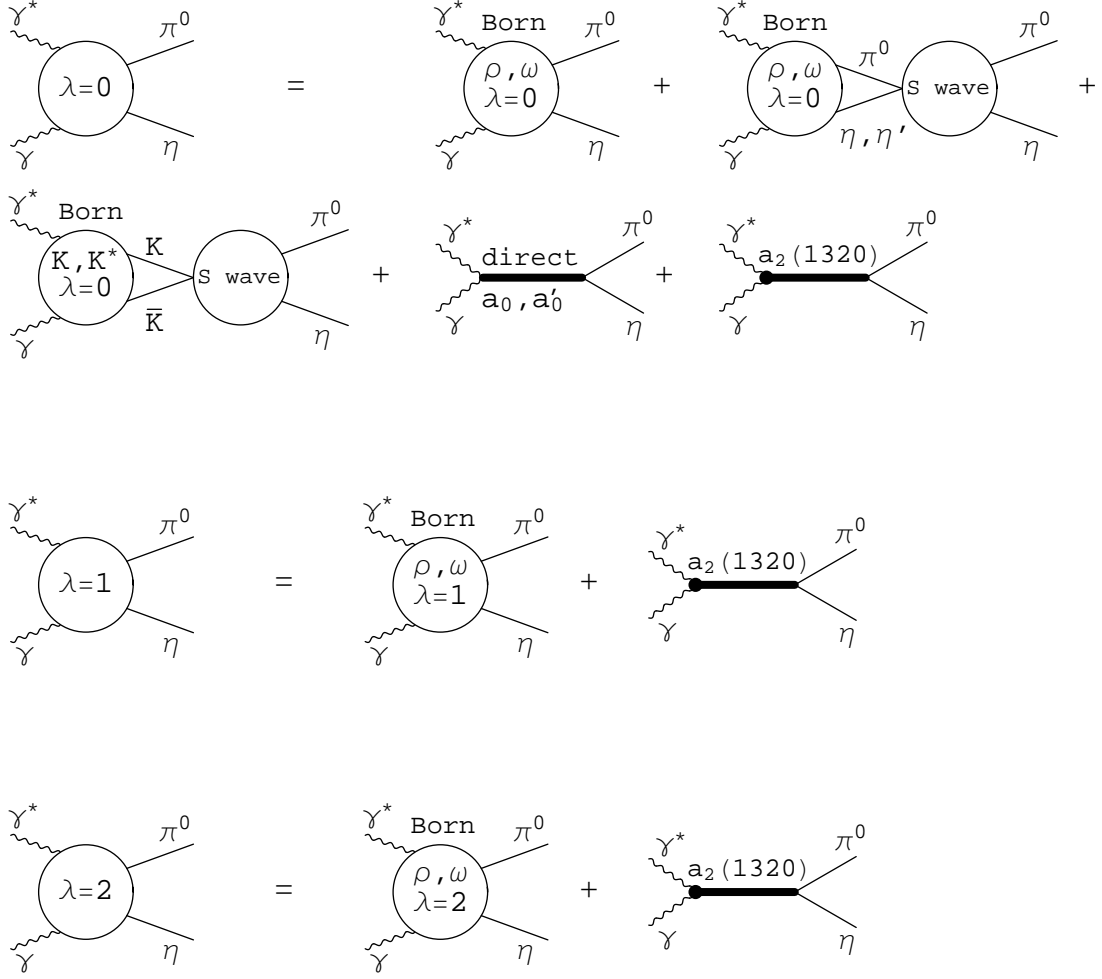


FIG. 1: Diagrammatical representation for the helicity amplitudes $\gamma^* \gamma \rightarrow \pi^0 \eta$.

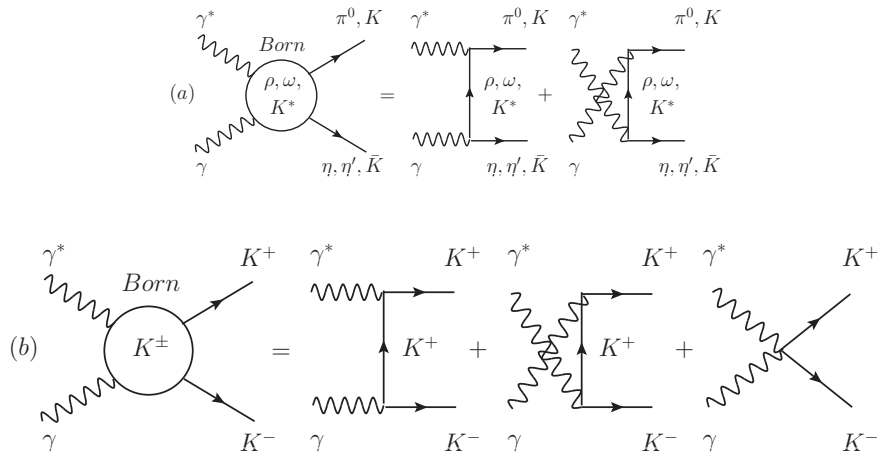


FIG. 2: The Born ρ, ω, K^*, K exchange diagrams for $\gamma^* \gamma \rightarrow \pi^0 \eta$, $\gamma^* \gamma \rightarrow \pi^0 \eta'$, and $\gamma^* \gamma \rightarrow K \bar{K}$.

Most of formulas in this section are modifications of Refs. [24, 25] results. In all diagrams the vector resonances undergo excitation in the γ^* line resulting in distinctive factors in the amplitudes.

According to Refs. [24, 25], we use a model for the helicity amplitudes M_λ (λ is the difference between photon helicities), taking into account electromagnetic Born contributions from ρ , ω , K^* , K exchanges and strong elastic and inelastic final-state interactions in $\pi^0\eta$, $\pi^0\eta'$, K^+K^- , and $K^0\bar{K}^0$ channels, as well as the contributions due to the direct interaction of the resonances with photons:

$$\begin{aligned}
M_0(\gamma^*\gamma \rightarrow \pi^0\eta; s, Q, \theta) &= M_0^{\text{Born } V}(\gamma^*\gamma \rightarrow \pi^0\eta; s, Q, \theta) + \tilde{I}_{\pi^0\eta}^V(s, Q) T_{\pi^0\eta \rightarrow \pi^0\eta}(s) \\
&+ \tilde{I}_{\pi^0\eta'}^V(s, Q) T_{\pi^0\eta' \rightarrow \pi^0\eta}(s) + \left(\tilde{I}_{K^+K^-}^{K^{*+}}(s, Q) - \tilde{I}_{K^0\bar{K}^0}^{K^{*0}}(s, Q) \right. \\
&\quad \left. + \tilde{I}_{K^+K^-}^{K^+}(s, Q) \right) T_{K^+K^- \rightarrow \pi^0\eta}(s) \\
&+ M_{\text{res}}^{\text{direct}}(s, Q) + M_0(\gamma^*\gamma \rightarrow a_2(1320) \rightarrow \pi^0\eta; s, Q, \theta), \tag{1}
\end{aligned}$$

$$\begin{aligned}
M_1(\gamma^*\gamma \rightarrow \pi^0\eta; s, Q, \theta) &= M_1^{\text{Born } V}(\gamma^*\gamma \rightarrow \pi^0\eta; s, Q, \theta) \\
&+ M_1(\gamma^*\gamma \rightarrow a_2(1320) \rightarrow \pi^0\eta; s, Q, \theta), \tag{2}
\end{aligned}$$

$$\begin{aligned}
M_2(\gamma^*\gamma \rightarrow \pi^0\eta; s, Q, \theta) &= M_2^{\text{Born } V}(\gamma^*\gamma \rightarrow \pi^0\eta; s, Q, \theta) \\
&+ M_2(\gamma^*\gamma \rightarrow a_2(1320) \rightarrow \pi^0\eta; s, Q, \theta), \tag{3}
\end{aligned}$$

the diagrams corresponding to these amplitudes are shown in Figs. 1, 2. Here θ is the angle between π^0 and γ (or η and γ^*) momenta in the $\gamma^*\gamma$ center-of-mass system.

The kaon loop contribution $\gamma^*\gamma \rightarrow K^+K^- \rightarrow a_0 \rightarrow \eta\pi^0$ (the term $\tilde{I}_{K^+K^-}^{K^+}(s, Q)T_{K^+K^- \rightarrow \pi^0\eta}(s)$) and the a_2 contribution are the largest ones, but other terms are also essential. I -functions are loop integrals, T -functions represent rescattering amplitudes (see below).

In the case of real photons $M_1(\gamma^*\gamma \rightarrow \pi^0\eta)$ vanishes because of the electromagnetic current conservation. The $M_0(\gamma^*\gamma \rightarrow a_2(1320) \rightarrow \pi^0\eta)$ is small at $Q = 0$ according to experiment.

The cross sections $\sigma_\lambda \equiv \sigma_\lambda(\gamma^*\gamma \rightarrow \eta\pi^0, s, Q)$ are related to the amplitudes M_λ as

$$\sigma_\lambda = \frac{\rho_{\pi\eta}(s)}{64\pi s \rho_{\gamma^*\gamma}} \int_{-0.8}^{0.8} |M_\lambda|^2 d\cos\theta, \quad \rho_{\gamma^*\gamma} = 1 + Q^2/s, \tag{4}$$

$$\bar{\sigma}_\lambda = \frac{1}{2a} \int_{\sqrt{s}-a}^{\sqrt{s}+a} \sigma_\lambda(s') d\sqrt{s'}, \quad (5)$$

and the total cross section $\sigma(\gamma^*(Q^2)\gamma \rightarrow \eta\pi^0, s) = \sigma_0 + \sigma_1 + \sigma_2$. The limits $|\cos\theta| \leq 0.8$ and bin size $2a = 20$ MeV were used in the experiment Ref. [28], where the data on the sum $\bar{\sigma}_0 + \bar{\sigma}_2$ at $Q = 0$ were presented for different values of \sqrt{s} ($\sigma_1 = \bar{\sigma}_1 = 0$ at $Q = 0$).

Let us derive all the terms in Eqs. (1), (2), and (3).

The Born term $M_\lambda^{\text{Born } V}$ is caused by equal [30] contributions of the ρ and ω exchange mechanisms [14]. It is calculated by Vector Dominance Model (VDM), the result is the significant modification of Eqs. (3) and (4) of Ref. [24]:

$$M_0^{\text{Born } V}(\gamma^*\gamma \rightarrow \pi^0\eta; s, Q, \theta) = 2g_{\omega\pi\gamma}g_{\omega\eta\gamma}F_{\eta\pi^0}^{\text{Born}}(Q) \left[\frac{A_0(s, t, Q, m_\eta, m_\pi)G_\omega(s, t)}{t - m_\omega^2} + \frac{A_0(s, u, Q, m_\pi, m_\eta)G_\omega(s, u)}{u - m_\omega^2} \right], \quad (6)$$

$$M_1^{\text{Born } V}(\gamma^*\gamma \rightarrow \pi^0\eta; s, Q, \theta) = 2g_{\omega\pi\gamma}g_{\omega\eta\gamma}F_{\eta\pi^0}^{\text{Born}}(Q) \left[\frac{A_1(s, t, Q, m_\eta, m_\pi)G_\omega(s, t)}{t - m_\omega^2} + \frac{A_1(s, u, Q, m_\pi, m_\eta)G_\omega(s, u)}{u - m_\omega^2} \right], \quad (7)$$

$$M_2^{\text{Born } V}(\gamma^*\gamma \rightarrow \pi^0\eta; s, Q, \theta) = \frac{2g_{\omega\pi\gamma}g_{\omega\eta\gamma}}{4}F_{\eta\pi^0}^{\text{Born}}(Q) \left(m_\eta^2 m_\pi^2 - tu + \frac{Q^2}{s + Q^2}(t - m_\pi^2)(u - m_\eta^2) \right) \left[\frac{G_\omega(s, t)}{t - m_\omega^2} + \frac{G_\omega(s, u)}{u - m_\omega^2} \right], \quad (8)$$

where

$$A_0(s, t, Q, m_1, m_2) = \frac{t(s + Q^2)}{4} + \frac{Q^2(t - m_2^2)^2}{4(s + Q^2)},$$

$$A_1(s, t, Q, m_1, m_2) = Q\sqrt{-t + \frac{(m_2^2 - m_1^2 - Q^2)^2}{4s}},$$

t and u are the Mandelstam variables for the reaction $\gamma^*\gamma \rightarrow \eta\pi^0$:

$$t = m_\pi^2 - \frac{1 + Q^2/s}{2} \left(s + m_\pi^2 - m_\eta^2 - s \rho_{\eta\pi^0} \cos\theta \right),$$

$$u = m_\eta^2 - \frac{1 + Q^2/s}{2} \left(s + m_\eta^2 - m_\pi^2 + s \rho_{\eta\pi^0} \cos\theta \right),$$

hereafter $\rho_{ab}(s) = 2p_{ab}(s)/\sqrt{s} = \sqrt{(1 - m_+^2/s)(1 - m_-^2/s)}$, $m_{\pm} = m_a \pm m_b$ ($ab = \eta\pi^0, K^+K^-, K^0\bar{K}^0, \eta'\pi^0$), where p_{ab} is the modulus of the momentum of a (or b) particles in the s.c.m., $g_{\omega\pi\gamma}^2 = 12\pi\Gamma_{\omega \rightarrow \pi\gamma}[(m_\omega^2 - m_\pi^2)/(2m_\omega)]^{-3} \approx 0.519 \text{ GeV}^{-2}$, $g_{\omega\eta\gamma}^2 = 12\pi\Gamma_{\omega \rightarrow \eta\gamma}[(m_\omega^2 - m_\eta^2)/(2m_\omega)]^{-3} \approx 1.86 \times 10^{-2} \text{ GeV}^{-2}$ [25]. The factor $F_{\eta\pi^0}^{\text{Born}}(Q)$ is due to vector resonances in the γ^* line and reads

$$F_{\eta\pi^0}^{\text{Born}}(Q) = \frac{1}{2} \left(\frac{1}{1 + Q^2/m_\rho^2} + \frac{1}{1 + Q^2/m_\omega^2} \right). \quad (9)$$

As in Refs. [24, 25], we take the formfactor $G_\omega(s, t) = G_\rho(s, t)$ of forms

$$G_\omega(s, t) = \exp[(t - m_\omega^2)b_\omega(s)], \quad (10)$$

$$b_\omega(s) = b_\omega^0 + (\alpha'_\omega/4) \ln[1 + (s/s_0)^4], \quad (11)$$

where $b_\omega^0 = 0$, $\alpha'_\omega = 0.8 \text{ GeV}^{-2}$, and $s_0 = 1 \text{ GeV}^2$. Form factors for the K^* exchange result from the above by substitution of m_{K^*} for m_ω , other parameters are the same.

The function $\tilde{I}_{\pi^0\eta}^V(s, Q)$ reads

$$\tilde{I}_{\pi^0\eta}^V(s, Q) = \frac{s}{\pi} \int_{(m_\eta + m_\pi)^2}^\infty ds' \rho_{\eta\pi}(s') \frac{M_{00}^{\text{Born } V}(\gamma^*\gamma \rightarrow \pi^0\eta; s, Q)}{s'(s' - s - i\varepsilon)}, \quad (12)$$

$$M_{00}^{\text{Born } V}(\gamma^*\gamma \rightarrow \pi^0\eta; s, Q) = \frac{1}{2} \int_{-1}^1 M_0^{\text{Born } V}(\gamma^*\gamma \rightarrow \pi^0\eta; s, Q, \theta) d\cos\theta. \quad (13)$$

The loop functions $\tilde{I}_{\pi^0\eta'}^V(s, Q)$, $\tilde{I}_{K^+K^-}^{K^{*+}}(s, Q)$ and $\tilde{I}_{K^0\bar{K}^0}^{K^{*0}}(s, Q)$ are built in a similar way. In the Born amplitudes for the $\gamma^*\gamma \rightarrow \pi^0\eta'$ process the constant $g_{\omega\eta'\gamma}^2 = 4\pi\Gamma_{\eta' \rightarrow \omega\gamma}[(m_{\eta'}^2 - m_\omega^2)/(2m_\omega)]^{-3} \approx 1.86 \times 10^{-2} \text{ GeV}^{-2}$ [1], also we have $F_{\eta'\pi^0}^{\text{Born}}(Q) = F_{\eta\pi^0}^{\text{Born}}(Q)$. The amplitudes $M_\lambda^{\text{Born } K^*}(\gamma^*\gamma \rightarrow K\bar{K}; s, \theta)$ for the K^* exchanges result from Eqs. (6), (7), (8) with the help of substitutions $m_\omega \rightarrow m_{K^*}$, $G_\omega \rightarrow G_{K^*}$, $m_\pi \rightarrow m_K$, $m_\eta \rightarrow m_K$, and $2g_{\omega\pi\gamma}g_{\omega\eta\gamma} \rightarrow g_{K^*K\gamma}^2$, where $g_{K^{*+}K^+\gamma}^2 \approx 0.064 \text{ GeV}^{-2}$ and $g_{K^{*0}K^0\gamma}^2 \approx 0.151 \text{ GeV}^{-2}$ [25]. The factors $F_{KK}^{\text{Born } K^{*+}}(Q)$ and $F_{KK}^{\text{Born } K^{*0}}(Q)$, provided by quark counting, are

$$F_{KK}^{\text{Born } K^{*+}}(Q) = \frac{3/2}{1 + Q^2/m_\rho^2} + \frac{1/2}{1 + Q^2/m_\omega^2} - \frac{1}{1 + Q^2/m_\phi^2}, \quad (14)$$

$$F_{KK}^{\text{Born } K^{*0}}(Q) = \frac{3/4}{1 + Q^2/m_\rho^2} - \frac{1/4}{1 + Q^2/m_\omega^2} + \frac{1/2}{1 + Q^2/m_\phi^2}. \quad (15)$$

The kaon loop integral $\tilde{I}_{K^+K^-}^{K^+}(s, Q)$ is

$$\begin{aligned} \tilde{I}_{K^+K^-}^{K^+}(s, Q) = & -F_{K^+}(Q)8\alpha \left\{ 1 + \frac{Q^2}{s+Q^2} \left(\rho_{K^+K^-}(s) \left(\ln \frac{1+\rho_{K^+K^-}(s)}{1-\rho_{K^+K^-}(s)} - i\pi \right) - \right. \right. \\ & \left. \left. \rho_{K^+K^-}(-Q^2) \ln \frac{1+\rho_{K^+K^-}(-Q^2)}{\rho_{K^+K^-}(-Q^2)-1} + \right. \right. \\ & \left. \left. \frac{m_{K^+}^2}{Q^2} \left(-\ln^2 \frac{1+\rho_{K^+K^-}(-Q^2)}{\rho_{K^+K^-}(-Q^2)-1} + \left(\ln \frac{1+\rho_{K^+K^-}(s)}{1-\rho_{K^+K^-}(s)} - i\pi \right)^2 \right) \right\}, \end{aligned} \quad (16)$$

$$F_{K^+}(Q) = \frac{1/2}{1+Q^2/m_\rho^2} + \frac{1/6}{1+Q^2/m_\omega^2} + \frac{1/3}{1+Q^2/m_\phi^2}. \quad (17)$$

The amplitudes of the pseudoscalar pairs rescattering are

$$T_{\pi^0\eta \rightarrow \pi^0\eta}(s) = T_0^1(s) = \frac{\eta_0^1(s)e^{2i\delta_0^1(s)} - 1}{2i\rho_{\pi\eta}(s)} = T_{\pi\eta}^{bg}(s) + e^{2i\delta_{\pi\eta}^{bg}(s)}T_{\pi^0\eta \rightarrow \pi^0\eta}^{res}(s), \quad (18)$$

$$T_{\pi^0\eta' \rightarrow \pi^0\eta}(s) = T_{\pi^0\eta' \rightarrow \pi^0\eta}^{res}(s) e^{i[\delta_{\pi\eta'}^{bg}(s) + \delta_{\pi\eta}^{bg}(s)]}, \quad (19)$$

$$T_{K^+K^- \rightarrow \pi^0\eta}(s) = T_{K^+K^- \rightarrow \pi^0\eta}^{res}(s) e^{i[\delta_{K\bar{K}}^{bg}(s) + \delta_{\pi\eta}^{bg}(s)]}, \quad (20)$$

where $T_{\pi\eta}^{bg}(s) = (e^{2i\delta_{\pi\eta}^{bg}(s)} - 1)/(2i\rho_{\pi\eta}(s))$, $T_{\pi^0\eta \rightarrow \pi^0\eta}^{res}(s) = (\eta_0^1(s)e^{2i\delta_{\pi\eta}^{res}(s)} - 1)/(2i\rho_{\pi\eta}(s))$, $\delta_0^1(s) = \delta_{\pi\eta}^{bg}(s) + \delta_{\pi\eta}^{res}(s)$, $\delta_{\pi\eta}^{bg}(s)$, $\delta_{\pi\eta'}^{bg}(s)$, and $\delta_{K\bar{K}}^{bg}(s)$ are the phase shifts of the elastic background contributions in the channels $\pi\eta$, $\pi\eta'$, and $K\bar{K}$ with isospin $I = 1$, respectively.

When a'_0 is taken into account the resonant amplitudes of the processes $ab \rightarrow \eta\pi^0$ are

$$T_{ab \rightarrow \eta\pi^0}^{res}(s) = \sum_{R,R'} \frac{g_{Rab}G_{RR'}^{-1}g_{R'\eta\pi^0}}{16\pi}, \quad (21)$$

where $R, R' = a_0, a'_0$ and pair $ab = \gamma\gamma, \eta\pi^0, K^+K, \eta'\pi^0$.

For $a, b \neq \gamma\gamma$ the constants g_{Rab} are related to the width

$$\Gamma_R(m) = \sum_{ab} \Gamma(R \rightarrow ab, m) = \sum_{ab} \frac{g_{Rab}^2}{16\pi m} \rho_{ab}(m). \quad (22)$$

In case of $ab = \gamma\gamma$ the constants $g_{R\gamma\gamma} \equiv g_{R\gamma\gamma}^{(0)}$ are related to the "direct" width as

$$\Gamma_{R \rightarrow \gamma\gamma}^{(0)} = \frac{|m_R^2 g_{R\gamma\gamma}^{(0)}|^2}{16\pi m_R}. \quad (23)$$

Remind that this is only a part of $R \rightarrow \gamma\gamma$ width, which is mainly produced by rescatterings.

The matrix of the inverse propagators [16] is

$$G_{RR'} \equiv G_{RR'}(m) = \begin{pmatrix} D_{a'_0}(m) & -\Pi_{a'_0 a_0}(m) \\ -\Pi_{a'_0 a_0}(m) & D_{a_0}(m) \end{pmatrix},$$

$$\Pi_{a'_0 a_0}(m) = \sum_{a,b} \frac{g_{a'_0 ab}}{g_{a_0 ab}} \Pi_{a_0}^{ab}(m) + C_{a'_0 a_0},$$

where m is the invariant mass of the $\eta\pi^0$ system, $m^2 = s$, the constant $C_{a'_0 a_0}$ incorporates the subtraction constant for the transition $a_0(980) \rightarrow (0^-0^-) \rightarrow a'_0$ and effectively takes into account contribution of multi-particle intermediate states to $a_0 \leftrightarrow a'_0$ transition, see Ref. [16]. The inverse propagator of the R scalar meson is presented also in Refs. [15, 16]:

$$D_R(m) = m_R^2 - m^2 + \sum_{ab} [Re\Pi_R^{ab}(m_R^2) - \Pi_R^{ab}(m^2)], \quad (24)$$

where $\sum_{ab} [Re\Pi_R^{ab}(m_R^2) - \Pi_R^{ab}(m^2)] = Re\Pi_R(m_R^2) - \Pi_R(m^2)$ takes into account the finite width corrections of the resonance which are the one loop contribution to the self-energy of the R resonance from the two-particle intermediate ab states.

Polarization operators of the a_0 and a'_0 are provided in Appendix I.

For the background phase shifts we use the parametrizations from Refs. [24, 25]:

$$e^{2i\delta_{ab}^{bg}(s)} = \frac{1 + iF_{ab}(s)}{1 - iF_{ab}(s)}, \quad (25)$$

where

$$F_{\pi\eta}(s) = \frac{\sqrt{1 - (m_\eta + m_\pi)^2/s} (c_0 + c_1 (s - (m_\eta + m_\pi)^2))}{1 + c_2 (s - (m_\eta + m_\pi)^2)^2}, \quad (26)$$

$$F_{K\bar{K}}(s) = f_{K\bar{K}} \sqrt{s - 4m_{K^+}^2}, \quad (27)$$

$$F_{\pi\eta'}(s) = f_{\pi\eta'} \sqrt{s - (m_{\eta'} + m_\pi)^2}. \quad (28)$$

Note that analytical continuation of the phases under the thresholds changes modules of corresponding amplitudes. The parameterization of $F_{K\bar{K}}(s)$ slightly differs from Refs. [24, 25].

The amplitude $M_{\text{res}}^{\text{direct}}(s, Q)$:

$$M_{\text{res}}^{\text{direct}}(s, Q) = 16\pi s T_{\gamma\gamma \rightarrow \eta\pi^0}^{\text{res}}(s) F^{\text{direct}}(s, Q) e^{i\delta_{\pi\eta}^{bg}(s)}, \quad (29)$$

$$F^{\text{direct}}(s, Q) = \frac{1}{2} \left(\frac{1}{1 + Q^2/m_\rho^2} + \frac{1}{1 + Q^2/m_\omega^2} \right) (1 + Q^2/s), \quad (30)$$

describes the $\gamma^*\gamma \rightarrow \pi^0\eta$ transition caused by the direct coupling constants of the a_0 and a'_0 resonances to photons $g_{a_0\gamma\gamma}^{(0)}$ and $g_{a'_0\gamma\gamma}^{(0)}$. $T_{\gamma\gamma \rightarrow \eta\pi^0}^{\text{res}}$ is defined in Eqs. (21) and (23), the factor $s(1 + Q^2/s)$ appears due to the gauge invariance (the effective Lagrangian $\sim F_{\mu\nu}F^{\mu\nu}a_0$, $M_{\text{res}}^{\text{direct}}(s, Q) \sim (kq)$).

It is known that in the reaction $\gamma\gamma \rightarrow a_2 \rightarrow \eta\pi$ tensor mesons are produced mainly by the photons with the opposite helicity states. The effective Lagrangian in this case is

$$\begin{aligned} L &= g_{a_2\gamma\gamma} T_{\mu\nu} F_{\mu\sigma} F_{\nu\sigma}, \\ F_{\mu\sigma} &= \partial_\mu A_\sigma - \partial_\sigma A_\mu, \end{aligned} \quad (31)$$

where A_μ is a photon field and $T_{\mu\nu}$ is a tensor a_2 field. So in the frame of Vector Dominance Model we assume that the effective Lagrangian of the reaction $a_2 \rightarrow V(1)V(2)$ is [31]:

$$\begin{aligned} L &= g_{a_2V(1)V(2)} T_{\mu\nu} F_{\mu\sigma}^{V(1)} F_{\nu\sigma}^{V(2)}, \\ F_{\mu\sigma}^{V(i)} &= \partial_\mu V(i)_\sigma - \partial_\sigma V(i)_\mu; \quad i = 1, 2. \end{aligned} \quad (32)$$

Matrix elements for $a_2(1320)$ contribution are in Ref. [31]:

$$M_2(\gamma^*\gamma \rightarrow a_2(1320) \rightarrow \pi^0\eta; s, Q, \theta) = A(s, Q) \sin^2 \theta, \quad (33)$$

$$M_1(\gamma^*\gamma \rightarrow a_2(1320) \rightarrow \pi^0\eta; s, Q, \theta) = -\sqrt{2}A(s, Q) \sqrt{\frac{Q^2}{s}} \sin \theta \cos \theta, \quad (34)$$

$$M_0(\gamma^*\gamma \rightarrow a_2(1320) \rightarrow \pi^0\eta; s, Q, \theta) = -A(s, Q) \frac{Q^2}{s} \left(\cos^2 \theta - \frac{1}{3} \right), \quad (35)$$

$$A(s, Q) = 20\pi F_{a_2}(Q) \sqrt{\frac{6s\Gamma_{a_2 \rightarrow \gamma\gamma}(s)\Gamma_{a_2 \rightarrow \eta\pi^0}(s)}{\rho_{\eta\pi^0}(s)}} \frac{1}{D_{a_2}(s)} \left(1 + \frac{Q^2}{s} \right). \quad (36)$$

The $F_{a_2}(Q)$ is defined and discussed in Sec. IV. The $F_{a_2}(0) = 1$, and the F_{a_2} dependence on Q does not influence on the $\gamma\gamma \rightarrow \eta\pi^0$ process. Note that Eq. (36) differs from Eq. (3) in Ref. [31] because of normalization of the amplitude and the sign of $g_{a_2\gamma\gamma}$, which is taken negative.

As in Refs. [24, 25] we take

$$D_{a_2}(m^2) = m_{a_2}^2 - m^2 - im\Gamma_{a_2}(m), \quad (37)$$

where

$$\Gamma_{a_2}(m) = \Gamma_{a_2}^{tot} \frac{m_{a_2}^2}{m^2} \frac{p_{\eta\pi}^5(m)}{p_{\eta\pi}^5(m_{a_2})} \frac{D_2(r_{a_2} p_{\eta\pi}(m_{a_2}))}{D_2(r_{a_2} p_{\eta\pi}(m))}, \quad (38)$$

and

$$\Gamma_{a_2 \rightarrow \eta\pi^0}(m) = Br(a_2 \rightarrow \eta\pi^0) \Gamma_{a_2}(m).$$

Here $D_2(x) = 9 + 3x^2 + x^4$ [32], and we take $m_{a_2} = 1318.3$ MeV, $\Gamma_{a_2}^{tot} = 105$ MeV, and $Br(a_2 \rightarrow \eta\pi^0) = 0.145$ from Ref. [1]. $\Gamma_{a_2 \rightarrow \gamma\gamma}(s) = (\sqrt{s}/m_{a_2})^3 \Gamma_{a_2 \rightarrow \gamma\gamma}(m_{a_2})$, $Br(a_2 \rightarrow \gamma\gamma) = 9.4 \times 10^{-6}$ [1]. We also take $r_{a_2} = 1.9$ GeV⁻¹ from Refs. [24, 25].

The $\phi \rightarrow \eta\pi^0\gamma$ decay description. Theoretical description of the KLOE data Ref. [20] on the mass spectrum $dBr(\phi \rightarrow \gamma\pi^0\eta, m)/dm$ is the same as in Ref. [21], with obvious change

$$\frac{g_{a_0 K^+ K^-} g_{a_0 \eta\pi^0}}{D_{a_0}(m)} \rightarrow \sum_{R, R'} g_{RK^+ K^-} G_{RR'}^{-1} g_{R' \eta\pi^0}. \quad (39)$$

The resulted formulas are in Appendix II.

III. RESULTS OF DATA DESCRIPTION

Using the above theoretical framework we fit the data Refs. [20, 28] and obtain results shown in Table I and Figs. 3, 4, and 5.

In Fit 1 the $m_{a'_0} = 1400$ MeV is in the middle of agreed corridor $\approx 1300 - 1500$ MeV [1], the a_0 coupling constant relations are close to the naive four-quark model predictions [15]:

$$\begin{aligned} g_{a_0 \eta\pi^0} &= \sqrt{2} \sin(\theta_p + \theta_q) g_{a_0 K^+ K^-} = (0.85 \div 0.98) g_{a_0 K^+ K^-}, \\ g_{a_0 \eta'\pi^0} &= -\sqrt{2} \cos(\theta_p + \theta_q) g_{a_0 K^+ K^-} = -(1.13 \div 1.02) g_{a_0 K^+ K^-}. \end{aligned} \quad (40)$$

In brackets first values correspond to $\theta_p = -18^\circ$ and the second ones to $\theta_p = -11^\circ$. The $\theta_q = 54.74^\circ$.

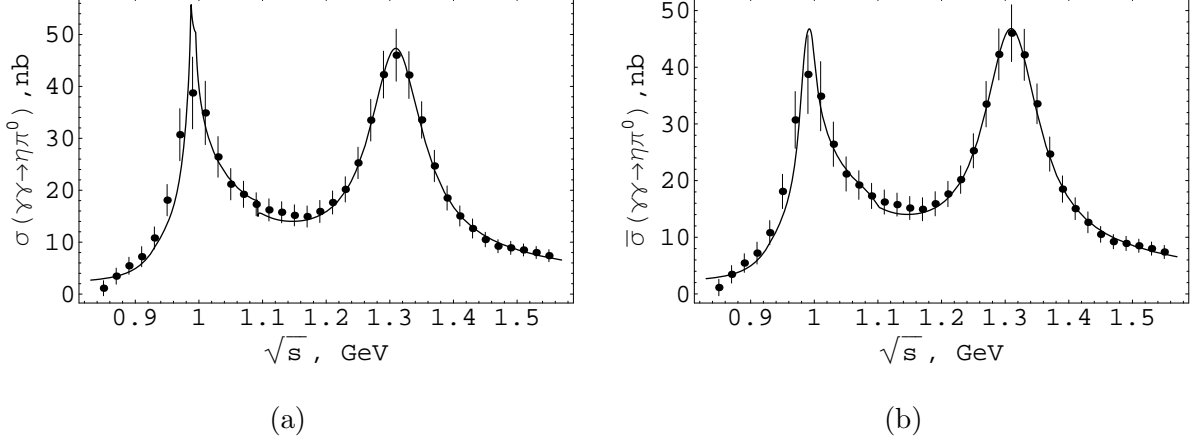


FIG. 3: The $\gamma\gamma \rightarrow \eta\pi^0$ cross section, $|\cos\theta| < 0.8$. The curves correspond to Fit 1, points are the Belle data [28]. The curve on the (a) figure represents cross section as is, while the curve on the (b) figure represents averaged cross section: each point of the curve is the cross section averaged over the ± 10 MeV neighborhood.

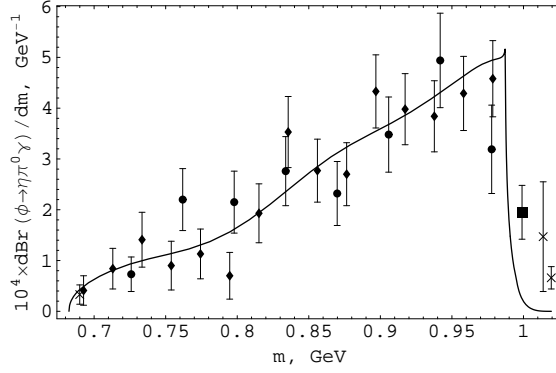


FIG. 4: Plot of the Fit 1 curve and the KLOE data (points) [20] on the $\phi \rightarrow \eta\pi^0\gamma$ decay. Cross points are omitted in fitting.

In Fit 1 the a_0 and a'_0 direct couplings with the $\gamma\gamma$ channel are close to their values in Refs. [24, 25].

One can see that the quality of experimental data description is good, see also Figs. 3, 4, and 5. This means that the data agree with the four-quark model scenario.

Fits 1, 3, and 4 are obtained with some restrictions, see Appendix III for details. Fit 2 is obtained without these restrictions by minimization of the χ^2 function only at $m_{a'_0} = 1400$ MeV. It shows that in the absence of restrictions the a_0 coupling constants go not too far from the four-quark model prediction and kaon loop gives main contribution to the $a_0 \rightarrow \gamma\gamma$

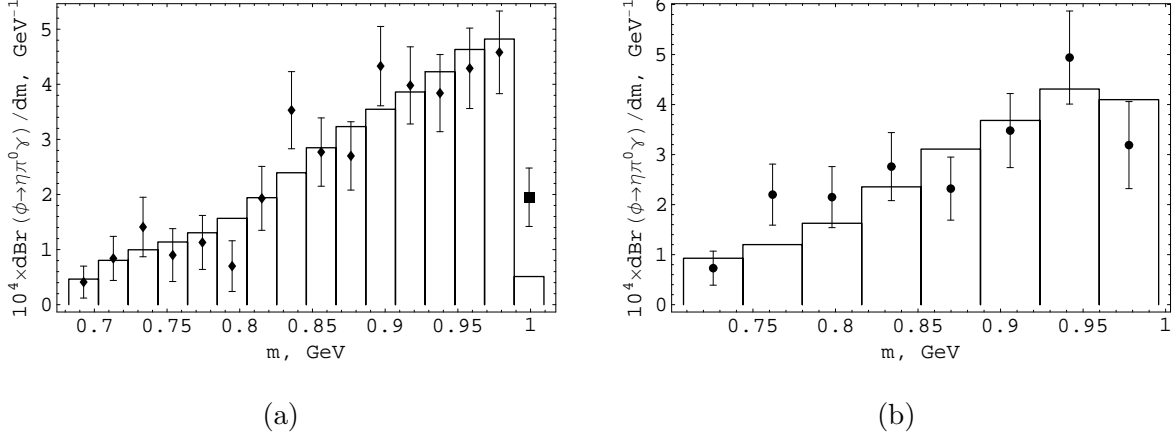


FIG. 5: The comparison of the KLOE data on $\phi \rightarrow \eta\pi^0\gamma$ decay and Fit 1. Histograms show Fit 1 curve averaged over each bin for (a) $\phi \rightarrow \eta\pi^0\gamma$, $\eta \rightarrow \gamma\gamma$ and (b) $\phi \rightarrow \eta\pi^0\gamma$, $\eta \rightarrow \pi^+\pi^-\pi^0$ samples, see details in Ref. [21].

width.

In Fits 3 and 4 the a'_0 mass $m_{a'_0}$ is set to 1300 MeV and 1500 MeV, respectively. Fits 3 and 4 show that the experimental data under consideration allow large range of $m_{a'_0}$ values. Note that it is possible to obtain good fits with $m_{a'_0} = 1200$ MeV and $m_{a'_0} = 1700$ MeV also [33].

Note also that both the data on $\gamma\gamma \rightarrow \eta\pi^0$ and the data on $\phi \rightarrow \eta\pi^0\gamma$ decay can be described without a'_0 contribution. But good $\gamma\gamma \rightarrow \eta\pi^0$ description (we achieved $\chi^2/n.d.f. = 15.1/27$) requires large width of the $a_0(980)$ ($\Gamma_{a_0}(m_{a_0}) \approx 650$ MeV, $\Gamma_{a_0}^{eff} \approx 100$ MeV), which contradicts the data on the $\phi \rightarrow \eta\pi^0\gamma$ decay (see also Ref. [21]).

The $g_{a_0\gamma\gamma}^{(0)}$ is caused by the $q\bar{q}$ component of the $a_0(980)$, $a_{2q}^0 = (u\bar{u} - d\bar{d})/\sqrt{2}$, while in the four-quark model [10] $a_{4q}^0 = (us\bar{u}\bar{s} - ds\bar{d}\bar{s})/\sqrt{2}$ decays to $\gamma\gamma$ only via loops. The obtained values of $g_{a_0\gamma\gamma}^{(0)}$ mean that the $\phi a_0\gamma$ point-like coupling constant $g_{\phi a_0\gamma}$ is negligible: the $g_{a_0\omega\gamma} \approx g_{a_0\gamma\gamma}^{(0)} \frac{f_\omega}{e}$, and $g_{a_0\phi\gamma}$ should be less than $g_{a_0\omega\gamma}$ at ~ 20 times because of $\phi - \omega$ mixing. Special fit with point-like contributions $g_{\phi a_0\gamma}$ and $g_{\phi a'_0\gamma}$ confirmed that it is not possible to extract these constants from the current data.

Note that the inverse sign of $g_{a_2\gamma\gamma}$ does not lead to essential consequences.

Table I. Properties of the resonances and main characteristics

| Fit | 1 | 2 | 3 | 4 |
|---|-------|--------|--------|--------|
| m_{a_0} , MeV | 993.9 | 994.5 | 995.3 | 988.7 |
| $g_{a_0 K^+ K^-}$, GeV | 2.75 | 2.43 | 3.87 | 3.71 |
| $g_{a_0 K^+ K^-}^2/4\pi$, GeV ² | 0.60 | 0.47 | 1.19 | 1.10 |
| $g_{a_0 \eta \pi}$, GeV | 2.74 | 3.09 | 3.69 | 3.61 |
| $g_{a_0 \eta \pi}^2/4\pi$, GeV ² | 0.60 | 0.76 | 1.09 | 1.04 |
| $g_{a_0 \eta' \pi}$, GeV | -2.86 | -4.62 | -4.15 | -3.95 |
| $g_{a_0 \eta' \pi}^2/4\pi$, GeV ² | 0.65 | 1.70 | 1.37 | 1.24 |
| $g_{a_0 \gamma \gamma}^{(0)}$, 10^{-3} GeV ⁻¹ | 1.8 | 2.7810 | 4.5919 | 3.2520 |
| $\Gamma_{a_0 \rightarrow \gamma \gamma}^{(0)}$, keV | 0.063 | 0.151 | 0.414 | 0.203 |
| $< \Gamma_{a_0 \rightarrow \gamma \gamma}^{direct} >_{\eta \pi^0}$, keV | 0.019 | 0.031 | 0.030 | 0.024 |
| $< \Gamma_{a_0 \rightarrow (K \bar{K} + \eta \pi^0 + \eta' \pi^0) \rightarrow \gamma \gamma} >_{\eta \pi^0}$, keV | 0.13 | 0.11 | 0.14 | 0.13 |
| $< \Gamma_{a_0 \rightarrow (K \bar{K} + \eta \pi^0 + \eta' \pi^0 + direct) \rightarrow \gamma \gamma} >_{\eta \pi^0}$, keV | 0.23 | 0.24 | 0.27 | 0.24 |
| $\Gamma_{a_0}(m_{a_0})$, MeV | 116.8 | 140.8 | 218.7 | 186.8 |
| $\Gamma_{a_0}^{eff}$, MeV | 34.6 | 57.2 | 38.8 | 44.8 |
| $m_{a'_0}$, MeV | 1400 | 1400 | 1300 | 1500 |
| $g_{a'_0 K^+ K^-}$, GeV | 1.63 | 0.26 | 0.93 | 2.36 |
| $g_{a'_0 K^+ K^-}^2/4\pi$, GeV ² | 0.21 | 0.005 | 0.07 | 0.44 |
| $g_{a'_0 \eta \pi}$, GeV | -3.12 | -1.49 | -2.55 | -2.82 |
| $g_{a'_0 \eta \pi}^2/4\pi$, GeV ² | 0.77 | 0.18 | 0.52 | 0.63 |
| $g_{a'_0 \eta' \pi}$, GeV | -4.75 | -7.19 | -5.20 | -5.77 |
| $g_{a'_0 \eta' \pi}^2/4\pi$, GeV ² | 1.80 | 4.12 | 2.15 | 2.64 |
| $g_{a'_0 \gamma \gamma}$, 10^{-3} GeV ⁻¹ | 5.5 | 9.927 | 8.2322 | 8.8103 |
| $\Gamma_{a'_0 \rightarrow \gamma \gamma}^{(0)}(m_{a'_0})$, keV | 1.7 | 5.4 | 3.0 | 5.2 |
| $\Gamma_{a'_0}(m_{a'_0})$, MeV | 330.9 | 399.4 | 271.0 | 453.4 |
| $C_{a_0 a'_0}$, GeV ² | 0.021 | 0.302 | -0.021 | -0.034 |

Table I (continuation).

| Fit | 1 | 2 | 3 | 4 |
|---|---------|---------|---------|---------|
| c_0 | 10.3 | 238.0 | 31.6 | 9.3 |
| c_1, GeV^{-2} | -24.2 | -554.8 | -76.6 | -22.9 |
| c_2, GeV^{-4} | -0.0009 | 96.1 | 14.6 | -0.0011 |
| $f_{K\bar{K}}, \text{GeV}^{-1}$ | -0.506 | -0.155 | 0.671 | 0.456 |
| $f_{\pi\eta'}, \text{GeV}^{-1}$ | 27.0 | 100.2 | 1.9 | 50.4 |
| $\delta, ^\circ$ | -94.5 | -132.0 | -166.3 | -144.3 |
| $\chi_{\gamma\gamma}^2 / 36 \text{ points}$ | 12.4 | 4.8 | 5.3 | 6.7 |
| $\chi_{sp}^2 / 24 \text{ points}$ | 24.5 | 24.7 | 24.1 | 24.3 |
| $(\chi_{\gamma\gamma}^2 + \chi_{sp}^2) / \text{n.d.f.}$ | 36.9/46 | 29.5/46 | 29.4/46 | 31.0/46 |

Remind that there should be no confusion due to relatively large a_0 width in Table I. The invariant mass spectrum of $\eta\pi^0$ in $a_0 \rightarrow \eta\pi^0$ is given by the relation

$$\frac{dN_{\eta\pi^0}}{dm} \sim \frac{2m^2}{\pi} \frac{\Gamma(a_0 \rightarrow \eta\pi^0, m)}{|D_{a_0}(m)|^2}. \quad (41)$$

The width of this distribution $\Gamma_{a_0}^{eff}$ is much less than the nominal width $\Gamma(a_0 \rightarrow \eta\pi^0, m_{a_0})$ due to strong $a_0 K\bar{K}$ coupling, usually $\Gamma_{a_0}^{eff}$ is 50 – 70 MeV, see Table I and Ref. [21].

Since the $a_0 \rightarrow \gamma\gamma$ amplitude changes rapidly near the $K\bar{K}$ threshold, it is reasonable to determine the effective width of the $a_0(980) \rightarrow \gamma\gamma$ decay averaged over the resonance mass distribution in the $\eta\pi^0$ channel [14, 24]:

$$\langle \Gamma_{a_0 \rightarrow \gamma\gamma} \rangle_{\eta\pi^0} = \int_{0.9 \text{ GeV}}^{1.1 \text{ GeV}} \frac{s}{4\pi^2} \sigma_0^{\text{res}}(\gamma\gamma \rightarrow \pi^0\eta; s) d\sqrt{s}, \quad (42)$$

where $\langle \Gamma_{a_0 \rightarrow \gamma\gamma} \rangle_{\eta\pi^0} \equiv \langle \Gamma_{a_0 \rightarrow (K\bar{K} + \eta\pi^0 + \eta'\pi^0 + \text{direct}) \rightarrow \gamma\gamma} \rangle_{\eta\pi^0}$, the integral is taken over the region occupied by the $a_0(980)$ resonance, and the σ_0^{res} is determined by the matrix element that contains only the resonance contributions from the rescatterings and direct transitions in Eq. (1), i.e. all contributions mentioned in Eq. (1) at $Q = 0$ except the Born one:

$$M_0^{\text{res}}(s) = \tilde{I}_{\pi^0\eta}^V(s, 0) T_{\pi^0\eta \rightarrow \pi^0\eta}(s) + \tilde{I}_{\pi^0\eta'}^V(s, 0) T_{\pi^0\eta' \rightarrow \pi^0\eta}(s) +$$

$$\left(\tilde{I}_{K^+K^-}^{K^{*+}}(s, 0) - \tilde{I}_{K^0\bar{K}^0}^{K^{*0}}(s, 0) + \tilde{I}_{K^+K^-}^{K^+}(s, 0) \right) T_{K^+K^- \rightarrow \eta\pi^0}(s) + M_{\text{res}}^{\text{direct}}(s, 0). \quad (43)$$

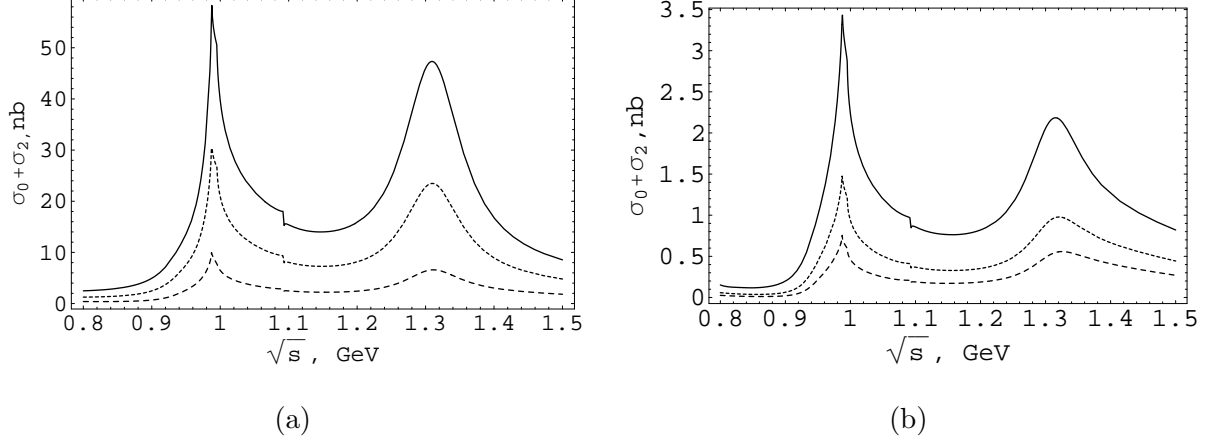


FIG. 6: The $\sigma_0(\gamma\gamma^*(Q^2) \rightarrow \eta\pi^0, s) + \sigma_2(\gamma\gamma^*(Q^2) \rightarrow \eta\pi^0, s)$, $|\cos\theta| < 0.8$, for Fit 1, $a = -0.08$ and $b = -0.15$. (a) Solid line $Q^2 = 0$, dashed line $Q^2 = 0.25 \text{ GeV}^2$, long-dashed line $Q^2 = 1 \text{ GeV}^2$; (b) Solid line $Q^2 = 2.25 \text{ GeV}^2$, dashed line $Q^2 = 4 \text{ GeV}^2$, long-dashed line $Q^2 = 6.25 \text{ GeV}^2$.

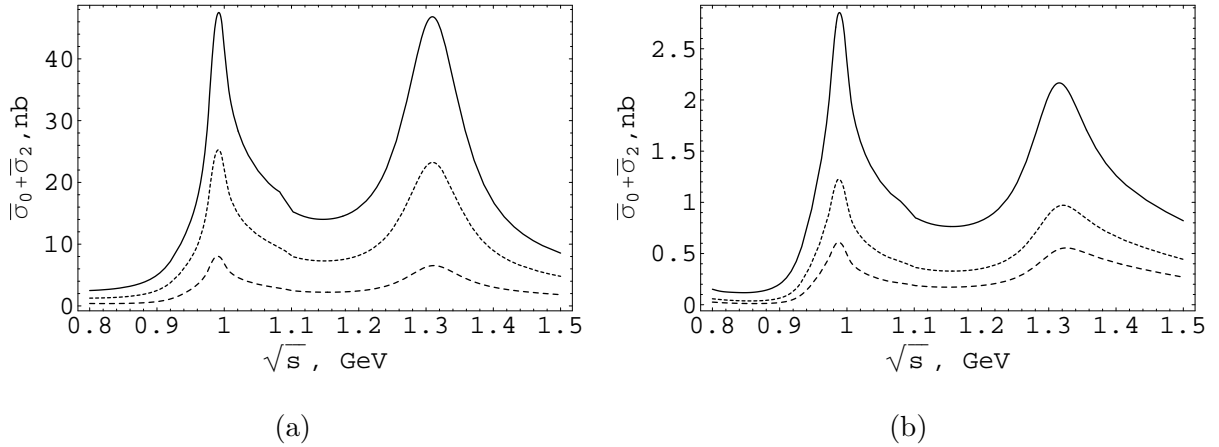


FIG. 7: The average $\gamma\gamma^*(Q^2) \rightarrow \eta\pi^0$ cross section, $|\cos\theta| < 0.8$, for the same parameters as in Fig. 6. Each point of the curve is the cross section averaged over the $\pm 10 \text{ MeV}$ neighborhood. (a) Solid line $Q^2 = 0$, dashed line $Q^2 = 0.25 \text{ GeV}^2$, long-dashed line $Q^2 = 1 \text{ GeV}^2$; (b) Solid line $Q^2 = 2.25 \text{ GeV}^2$, dashed line $Q^2 = 4 \text{ GeV}^2$, long-dashed line $Q^2 = 6.25 \text{ GeV}^2$.

This quantity is an adequate characteristic of the coupling of the $a_0(980)$ resonance with a $\gamma\gamma$ pair. One can also consider particular contributions to $\langle \Gamma_{a_0 \rightarrow \gamma\gamma} \rangle_{\eta\pi^0}$. The obtained results for $\langle \Gamma_{a_0 \rightarrow \gamma\gamma}^{direct} \rangle_{\eta\pi^0}$, $\langle \Gamma_{a_0 \rightarrow (K\bar{K} + \eta\pi^0 + \eta'\pi^0) \rightarrow \gamma\gamma} \rangle_{\eta\pi^0}$, and $\langle \Gamma_{a_0 \rightarrow (K\bar{K} + \eta\pi^0 + \eta'\pi^0 + direct) \rightarrow \gamma\gamma} \rangle_{\eta\pi^0}$ are shown in Table I. One can see that the averaged values are much less than the values at $m = m_{a_0}$, for example, $\langle \Gamma_{a_0 \rightarrow \gamma\gamma}^{direct} \rangle_{\eta\pi^0}$ is at 3-10 times less than $\Gamma_{a_0 \rightarrow \gamma\gamma}^{(0)}$ depending on fit.

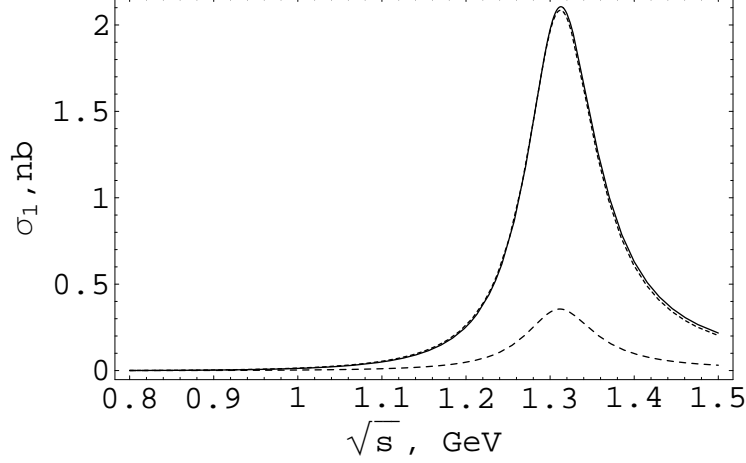


FIG. 8: The $\sigma_1(\gamma\gamma^*(Q^2) \rightarrow \eta\pi^0, s)$, $|\cos\theta| < 0.8$, for the same parameters as in Fig. 6. Solid line $Q^2 = 0.25 \text{ GeV}^2$, dashed line $Q^2 = 1 \text{ GeV}^2$, long-dashed line $Q^2 = 6.25 \text{ GeV}^2$.

IV. NON-ZERO Q

At $Q \rightarrow \infty$ the matrix elements in Eqs. (1), (2), and (3) have the following asymptotics. The $M_\lambda^{\text{Born } V}$ fall exponentially because of factor Eq. (10), the kaon loop contribution $\tilde{I}_{K^+K^-}^{K^+}(s, Q)T_{K^+K^- \rightarrow \pi^0\eta}(s)$ is $\sim \ln(Q^2/m_{K^+}^2)/Q^2$ [34]. The direct $a_0 \rightarrow \gamma^*\gamma$ interaction Eq. (29) does not depend on Q , this is similar to QCD based asymptotics Refs. [35, 36] for a scalar $q\bar{q}$ meson transition to $\gamma^*\gamma$. The obtained asymptotics for the kaon loop contribution $\sim 1/Q^2$ is similar to the QCD asymptotics for the scalar four-quark meson transition to $\gamma^*\gamma$. This emphasizes that the direct transition goes through the $q\bar{q}$ component of the a_0 , and the kaon loop involves the four-quark component of the a_0 .

For the $\gamma^*\gamma \rightarrow a_2$ transition the obtained asymptotics are

$$M_0(\gamma^*\gamma \rightarrow a_2) \sim F_{a_2}(Q)Q^4, \quad (44)$$

$$M_1(\gamma^*\gamma \rightarrow a_2) \sim F_{a_2}(Q)Q^3, \quad (45)$$

$$M_2(\gamma^*\gamma \rightarrow a_2) \sim F_{a_2}(Q)Q^2. \quad (46)$$

The hierarchy $M_0 : M_1 : M_2 = Q^2 : Q : 1$ is the consequence of the Lagrangian Eq. (32) and agrees with the QCD based prediction $M_\lambda(\gamma^*\gamma \rightarrow a_2) \sim Q^{-\lambda}$ [35, 36]. To reach this asymptotics one has to conclude that $F_{a_2}(Q) \sim 1/Q^4$, which is possible when vector excitations ρ' , ρ'' , ω' , and ω'' are taken into account. Basing on Ref. [27], let us take $F_{a_2}(Q) = \tilde{F}_{a_2}(Q)/\tilde{F}_{a_2}(0)$, where

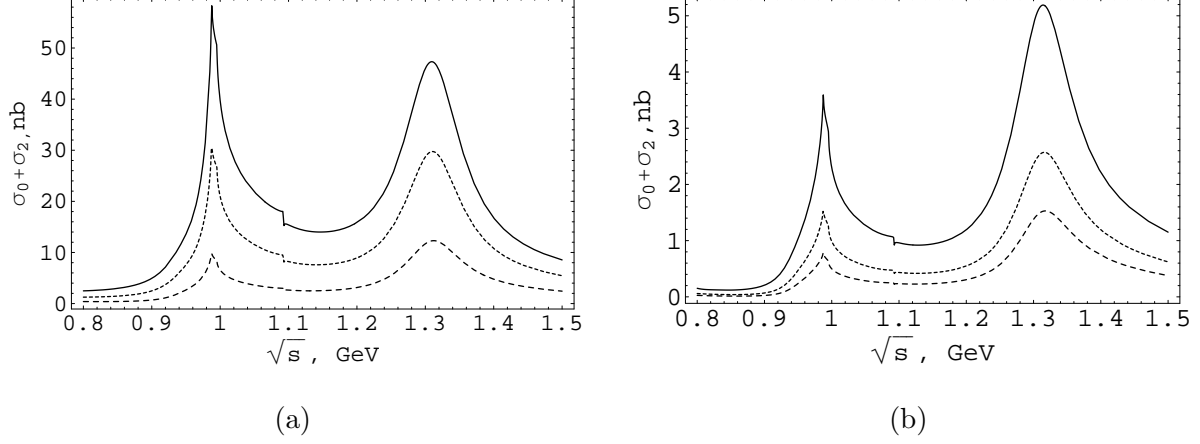


FIG. 9: The $\sigma_0(\gamma\gamma^*(Q^2) \rightarrow \eta\pi^0, s) + \sigma_2(\gamma\gamma^*(Q^2) \rightarrow \eta\pi^0, s)$, $|\cos\theta| < 0.8$, for Fit 1, $a = 3.84$ and $b = -3$. (a) Solid line $Q^2 = 0$, dashed line $Q^2 = 0.25 \text{ GeV}^2$, long-dashed line $Q^2 = 1 \text{ GeV}^2$; (b) Solid line $Q^2 = 2.25 \text{ GeV}^2$, dashed line $Q^2 = 4 \text{ GeV}^2$, long-dashed line $Q^2 = 6.25 \text{ GeV}^2$.

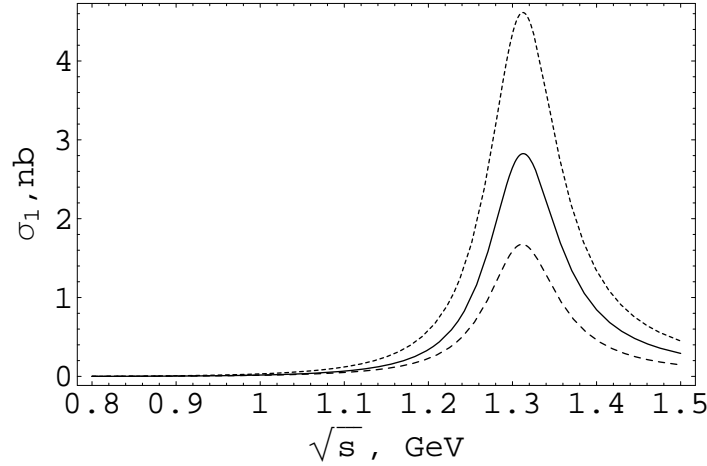


FIG. 10: The $\sigma_1(\gamma\gamma^*(Q^2) \rightarrow \eta\pi^0, s)$, $|\cos\theta| < 0.8$, for the same parameters as in Fig. 9. Solid line $Q^2 = 0.25 \text{ GeV}^2$, dashed line $Q^2 = 1 \text{ GeV}^2$, long-dashed line $Q^2 = 6.25 \text{ GeV}^2$.

$$\begin{aligned}
\tilde{F}_{a_2}(Q) &= \frac{g_{a_2\rho\omega}}{f_\rho f_\omega} \left(\frac{1}{1 + Q^2/m_\rho^2} + \frac{1}{1 + Q^2/m_\omega^2} \right) + \frac{g_{a_2\rho'\omega'}}{f_{\rho'} f_{\omega'}} \left(\frac{1}{1 + Q^2/m_{\rho'}^2} + \frac{1}{1 + Q^2/m_{\omega'}^2} \right) \\
&+ \frac{g_{a_2\rho''\omega''}}{f_{\rho''} f_{\omega''}} \left(\frac{1}{1 + Q^2/m_{\rho''}^2} + \frac{1}{1 + Q^2/m_{\omega''}^2} \right) = \frac{g_{a_2\rho\omega}}{f_\rho f_\omega} \left(\frac{1}{1 + Q^2/m_\rho^2} + \frac{1}{1 + Q^2/m_\omega^2} \right) \\
&+ a \left(\frac{1}{1 + Q^2/m_{\rho'}^2} + \frac{1}{1 + Q^2/m_{\omega'}^2} \right) + b \left(\frac{1}{1 + Q^2/m_{\rho''}^2} + \frac{1}{1 + Q^2/m_{\omega''}^2} \right). \quad (47)
\end{aligned}$$

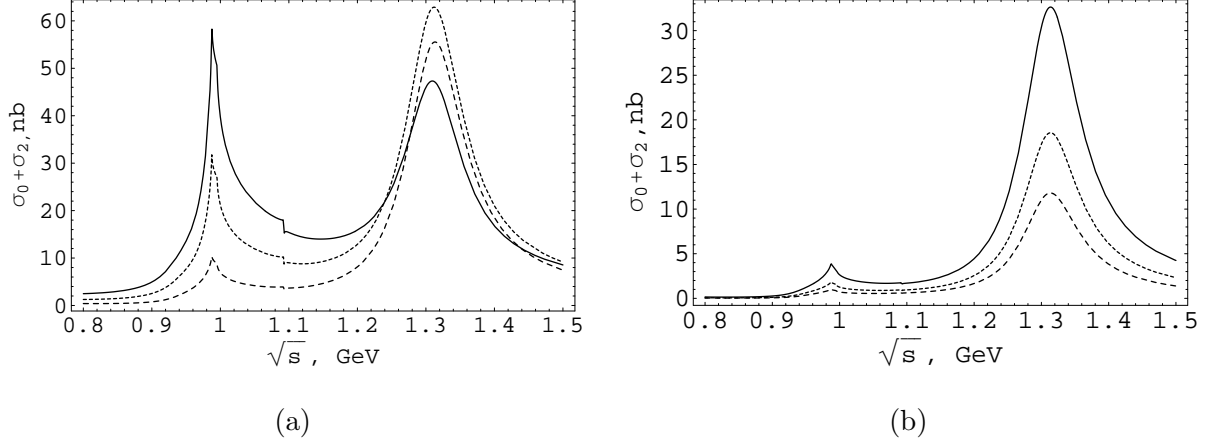


FIG. 11: The $\sigma_0(\gamma\gamma^*(Q^2) \rightarrow \eta\pi^0, s) + \sigma_2(\gamma\gamma^*(Q^2) \rightarrow \eta\pi^0, s)$, $|\cos\theta| < 0.8$, for Fit 1, $a = -4.41$ and $b = 3$. (a) Solid line $Q^2 = 0$, dashed line $Q^2 = 0.25 \text{ GeV}^2$, long-dashed line $Q^2 = 1 \text{ GeV}^2$; (b) Solid line $Q^2 = 2.25 \text{ GeV}^2$, dashed line $Q^2 = 4 \text{ GeV}^2$, long-dashed line $Q^2 = 6.25 \text{ GeV}^2$.

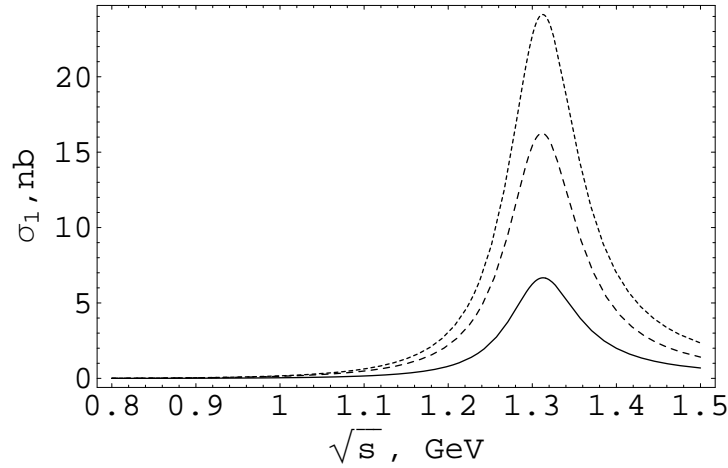


FIG. 12: The $\sigma_1(\gamma\gamma^*(Q^2) \rightarrow \eta\pi^0, s)$, $|\cos\theta| < 0.8$, for the same parameters as in Fig. 11. Solid line $Q^2 = 0.25 \text{ GeV}^2$, dashed line $Q^2 = 1 \text{ GeV}^2$, long-dashed line $Q^2 = 6.25 \text{ GeV}^2$.

Here $a = g_{a_2\rho'\omega'}f_\rho f_\omega / g_{a_2\rho\omega}f_{\rho'}f_{\omega'}$ and $b = g_{a_2\rho''\omega''}f_\rho f_\omega / g_{a_2\rho\omega}f_{\rho''}f_{\omega''}$. The requirement

$$m_\rho^2 + m_\omega^2 + a(m_{\rho'}^2 + m_{\omega'}^2) + b(m_{\rho''}^2 + m_{\omega''}^2) = 0 \quad (48)$$

leads to elimination of the contribution proportional to $1/Q^2$, so $F_{a_2}(Q)$ is $\sim 1/Q^4$ satisfying the QCD based asymptotics. This asymptotics is a manifestation of the radial vector excitations.

The requirement Eq. (48) do not fix both a and b . The ratio a/b is the question for the

experiment.

In the $\gamma^*(Q^2)\gamma \rightarrow f_2(1270) \rightarrow \pi^0\pi^0$ reaction the situation with asymptotics and cancellation due to radial vector excitations is similar.

Let us take in Eq. (47) $m_{\rho'} = m_{\omega'} = 1450$ MeV and $m_{\rho''} = m_{\omega''} = 1700$ MeV in agreement with Ref. [1].

If one takes $a = -0.08, b = -0.15$ together with the parameters of Fit 1, the a_0 and a_2 peaks fall synchronously with Q increase, see Figs. 6 and 7, where the sums $\sigma_0 + \sigma_2 \equiv \sigma_0(s, Q^2) + \sigma_2(s, Q^2)$ and $\bar{\sigma}_0 + \bar{\sigma}_2 \equiv \bar{\sigma}_0(s, Q^2) + \bar{\sigma}_2(s, Q^2)$ are shown for different values of Q^2 . The a_2 peak starts dominating only at $Q \sim 5$ GeV. The σ_1 is shown for different values of Q^2 in Fig. 8. In this case contribution of vector excitations is relatively small at $Q = 0$ as one could expect from general considerations.

Eqs. (47), (48) also contain cases when contribution of vector excitations exceeds the ρ and ω one even at $Q = 0$. Let us consider two of them.

In case $a = 3.84$ and $b = -3$ the a_0 and a_2 peaks in $\sigma_0 + \sigma_2$ fall synchronously for $Q < 1$ GeV, then the a_2 peak starts dominating, see Fig. 9. The σ_1 for this case is shown in Fig. 10.

The choice $a = -4.41$ and $b = 3$ leads to Fig. 11: the a_2 peak grows at low Q and falls under the value at $Q = 0$ only at $Q > 1$ GeV. Starting from $Q \approx 0.5$ GeV the a_2 peak dominates over the a_0 peak, see Fig. 11. The σ_1 is shown in Fig. 12.

We don't consider scenarios which seem doubtful. For example, for vast region of a and b the $F_{a_2}(Q_0) = 0$ at some $Q_0 < 1$ GeV.

Note that variation of the parameters in Table I do not provide such dramatic changes at $Q > 0$ as possible variation of a and b .

New Belle experiment could clarify what scenario is realized.

How vector excitations influence on contributions to the $\gamma\gamma \rightarrow \eta\pi^0$ amplitude not involving the a_2 meson is the question for separate investigation. The kaon loop contribution probably does not change dramatically because the couplings of the radial vector excitations with kaon channel, obtained in [37], are small. Other contributions are not so large. The direct transition $M_{\text{res}}^{\text{direct}}$ is small in agreement with the four-quark model scenario.

V. CONCLUSION

The experimental data on the $\gamma\gamma \rightarrow \eta\pi^0$ reaction evidence in favor of the four-quark model of the $a_0(980)$. The data is well described with the scenario based on four-quark model: relations Eqs. (40) and small $g_{a_0\gamma\gamma}^{(0)}$. The obtained values of $g_{a_0\gamma\gamma}^{(0)}$ mean that the $a_0\phi\gamma$ point-like coupling gives negligible contribution to $\phi \rightarrow \eta\pi^0\gamma$ process. The production (and decay) of the $a_0(980)$ via rescatterings, i.e. via the four-quark transitions, is the main qualitative argument in favour of the four-quark nature of the $a_0(980)$.

The Q^2 dependence of the cross section obtained with specific values of a and b (for example, shown in Figs. 6, 7 and 8) may be quite reliable in the region $Q < 1\text{--}2$ GeV [31]. At higher Q the obtained dependence may be treated only as a guide. Note that at very high Q one should use QCD.

The strong influence of radial vector excitations at $Q \sim 1$ GeV is considered also, see Figs. 9-12.

We don't use the kaon formfactor $G_{K^+}(t, u)$, introduced in Refs. [24, 25], since the data can be explained without it, and the processes $\phi \rightarrow \eta\pi^0\gamma$ as well as $\phi \rightarrow \pi^0\pi^0\gamma$ are described without this factor too.

As for comparative production of a_0 and a_2 in $\sigma_0 + \sigma_2$, at high $Q \gtrsim 5$ GeV the a_2 contribution dominates in all variants. In the intermediate region $Q \sim 1$ GeV the a_0 and a_2 peaks fall synchronously if vector excitations contribution is relatively small at $Q = 0$ as one could expect from general considerations. But in principle it is not excluded that the a_2 peak dominates in the intermediate region too, see Figs. 9, 11.

The data on $\gamma^*(Q^2)\gamma \rightarrow \pi^0\pi^0$ have recently appeared [38]. The perspectives of study of the $f_0(980)$ and $f_2(1270)$ comparative production in this reaction are poor because the $f_0(980)$ peak is considerably less than the $f_2(1270)$ peak in $\gamma\gamma \rightarrow \pi^0\pi^0$ already [25, 39]. As it was mentioned above, the mechanism of $f_2(1270)$ production in the reaction $\gamma^*(Q^2)\gamma \rightarrow f_2(1270)$ is similar to the mechanism of $a_2(1320)$ production in the process $\gamma^*(Q^2)\gamma \rightarrow a_2(1320)$. In Ref. [40], we considered in detail the changeover of the dominant helicity amplitude in the processes $\gamma^*(Q^2)\gamma \rightarrow f_2(1270)$ and $\gamma^*(Q^2)\gamma \rightarrow a_2(1320)$ with increasing Q^2 and showed that data from Ref. [38] could be satisfactorily described even with only one radial excitation (ρ').

Emphasize that the best process to study the a_2 production is the $\gamma^*(Q^2)\gamma \rightarrow a_2 \rightarrow \rho\pi$

reaction because $Br(a_2 \rightarrow \rho\pi) = 70\%$ [1] and the background is expected to be small.

The forthcoming SuperKEKB factory, which will have the luminosity at 40 times more than the KEKB one [1], could be the best place for investigation of the scalar and tensor mesons in $\gamma^*\gamma$ collisions.

VI. ACKNOWLEDGEMENTS

This work was supported in part by the Russian Foundation for Basic Research (Grants Nos. 13-02-00039 and 16-02-00065) and Interdisciplinary Project No. 102 of the Siberian Branch, Russian Academy of Sciences.

VII. APPENDIX I: POLARIZATION OPERATORS OF THE a_0 AND a'_0

For pseudoscalar a, b mesons and $m_a \geq m_b$, $m \geq m_+$ one has:

$$\begin{aligned} \Pi_R^{ab}(m^2) = & \frac{g_{Rab}^2}{16\pi} \left[\frac{m_+ m_-}{\pi m^2} \ln \frac{m_b}{m_a} + \right. \\ & \left. + \rho_{ab} \left(i + \frac{1}{\pi} \ln \frac{\sqrt{m^2 - m_-^2} - \sqrt{m^2 - m_+^2}}{\sqrt{m^2 - m_-^2} + \sqrt{m^2 - m_+^2}} \right) \right]. \end{aligned} \quad (49)$$

For $m_- \leq m < m_+$

$$\begin{aligned} \Pi_R^{ab}(m^2) = & \frac{g_{Rab}^2}{16\pi} \left[\frac{m_+ m_-}{\pi m^2} \ln \frac{m_b}{m_a} - |\rho_{ab}(m)| + \right. \\ & \left. + \frac{2}{\pi} |\rho_{ab}(m)| \arctan \frac{\sqrt{m_+^2 - m^2}}{\sqrt{m^2 - m_-^2}} \right], \end{aligned} \quad (50)$$

for $m < m_-$

$$\begin{aligned} \Pi_R^{ab}(m^2) = & \frac{g_{Rab}^2}{16\pi} \left[\frac{m_+ m_-}{\pi m^2} \ln \frac{m_b}{m_a} - \right. \\ & \left. - \frac{1}{\pi} \rho_{ab}(m) \ln \frac{\sqrt{m_+^2 - m^2} - \sqrt{m_-^2 - m^2}}{\sqrt{m_+^2 - m^2} + \sqrt{m_-^2 - m^2}} \right]. \end{aligned} \quad (51)$$

Note that we take into account intermediate states $\eta\pi^0, K\bar{K}, \eta'\pi^0$ in the $a_0(980)$ and a'_0 propagators:

$$\Pi_{a_0} = \Pi_{a_0}^{\eta\pi^0} + \Pi_{a_0}^{K^+K^-} + \Pi_{a_0}^{K^0\bar{K}^0} + \Pi_{a_0}^{\eta'\pi^0}, \quad (52)$$

and the same for a'_0 . Note that $g_{a_0 K^+ K^-} = -g_{a_0 K^0 \bar{K}^0}$ and $g_{a'_0 K^+ K^-} = -g_{a'_0 K^0 \bar{K}^0}$.

VIII. APPENDIX II: THE $\eta\pi^0$ SPECTRUM IN $\phi \rightarrow \eta\pi^0\gamma$ DECAY

The amplitude of the signal process $\phi(p) \rightarrow \gamma(a_0 + a'_0) \rightarrow \gamma(q)\pi^0(k_1)\eta(k_2)$ is

$$M_{sig} = e^{i\delta_B} g(m) \sum_{R,R'} g_{RK^+K^-} G_{RR'}^{-1} g_{R'\eta\pi^0} \left((\phi\epsilon) - \frac{(\phi q)(\epsilon p)}{(pq)} \right), \quad (53)$$

where $m^2 = (k_1 + k_2)^2$, ϕ_α and ϵ_μ are the polarization vectors of ϕ meson and photon, the function $g(m)$ is given below. The $\delta_B = \delta_{\eta\pi^0}^{bg} + \delta_{K\bar{K}}^{bg}$.

The matrix element of the background process $\phi(p) \rightarrow \pi^0\rho^0 \rightarrow \gamma(q)\pi^0(k_1)\eta(k_2)$ is

$$M_B = \frac{g_{\phi\rho\pi} g_{\rho\eta\gamma}}{D_\rho(p - k_1)} \phi_\alpha k_{1\mu} p_\nu \epsilon_\delta (p - k_1)_\omega q_\epsilon \epsilon_{\alpha\beta\mu\nu} \epsilon_{\beta\delta\omega\epsilon}. \quad (54)$$

The mass spectrum is

$$\frac{d\Gamma(\phi \rightarrow \gamma\pi^0\eta, m)}{dm} = \frac{d\Gamma_{sig}(m)}{dm} + \frac{d\Gamma_{back}(m)}{dm} + \frac{d\Gamma_{int}(m)}{dm}, \quad (55)$$

where the mass spectrum for the signal is

$$\frac{d\Gamma_{sig}(m)}{dm} = \frac{2|g(m)|^2 p_{\eta\pi}(m_\phi^2 - m^2)}{3(4\pi)^3 m_\phi^3} \left| \sum_{R,R'} g_{RK^+K^-} G_{RR'}^{-1} g_{R'\eta\pi^0} \right|^2. \quad (56)$$

The mass spectrum for the background process $\phi \rightarrow \pi^0\rho \rightarrow \gamma\pi^0\eta$ is [19]:

$$\frac{d\Gamma_{back}(m)}{dm} = \frac{(m_\phi^2 - m^2) p_{\pi\eta}}{128\pi^3 m_\phi^3} \int_{-1}^1 dx A_{back}(m, x), \quad (57)$$

where

$$\begin{aligned} A_{back}(m, x) &= \frac{1}{3} \sum |M_B|^2 = \\ &= \frac{1}{24} (m_\eta^4 m_\pi^4 + 2m^2 m_\eta^2 m_\pi^2 \tilde{m}_\rho^2 - 2m_\eta^4 m_\pi^2 \tilde{m}_\rho^2 - 2m_\eta^2 m_\pi^4 \tilde{m}_\rho^2 + \\ &2m^4 \tilde{m}_\rho^4 - 2m^2 m_\eta^2 \tilde{m}_\rho^4 + m_\eta^4 \tilde{m}_\rho^4 - 2m^2 m_\pi^2 \tilde{m}_\rho^4 + 4m_\eta^2 m_\pi^2 \tilde{m}_\rho^4 + m_\pi^4 \tilde{m}_\rho^4 + \\ &2m^2 \tilde{m}_\rho^6 - 2m_\eta^2 \tilde{m}_\rho^6 - 2m_\pi^2 \tilde{m}_\rho^6 + \tilde{m}_\rho^8 - 2m_\eta^4 m_\pi^2 m_\phi^2 - 2m^2 m_\eta^2 m_\phi^2 \tilde{m}_\rho^2 + \\ &2m_\eta^2 m_\pi^2 m_\phi^2 \tilde{m}_\rho^2 - 2m^2 m_\phi^2 \tilde{m}_\rho^4 + 2m_\eta^2 m_\phi^2 \tilde{m}_\rho^4 - 2m_\phi^2 \tilde{m}_\rho^6 + m_\eta^4 m_\phi^4 + m_\phi^4 \tilde{m}_\rho^4) \times \\ &\left| \frac{g_{\phi\rho\pi} g_{\rho\eta\gamma}}{D_\rho(\tilde{m}_\rho)} \right|^2, \end{aligned} \quad (58)$$

and

$$\begin{aligned}\tilde{m}_\rho^2 &= m_\eta^2 + \frac{(m^2 + m_\eta^2 - m_\pi^2)(m_\phi^2 - m^2)}{2m^2} - \frac{(m_\phi^2 - m^2)x}{m} p_{\pi\eta} \\ p_{\pi\eta} &= \frac{\sqrt{(m^2 - (m_\eta - m_\pi)^2)(m^2 - (m_\eta + m_\pi)^2)}}{2m}.\end{aligned}\quad (59)$$

The term of the interference between the signal and the background processes is written in the following way:

$$\frac{d\Gamma_{int}(m)}{dm} = \frac{(m_\phi^2 - m^2)p_{\pi\eta}}{128\pi^3 m_\phi^3} \int_{-1}^1 dx A_{int}(m, x), \quad (60)$$

where

$$\begin{aligned}A_{int}(m, x) &= \frac{2}{3} Re \sum M_{sig} M_B^* = \frac{1}{3} \left((m^2 - m_\phi^2) \tilde{m}_\rho^2 + \frac{m_\phi^2 (\tilde{m}_\rho^2 - m_\eta^2)^2}{m_\phi^2 - m^2} \right) \times \\ &Re \left\{ \frac{e^{i\delta} g(m) \left(\sum_{R,R'} g_{RK+K-} G_{RR'}^{-1} g_{R'\eta\pi^0} \right) g_{\phi\rho\pi} g_{\rho\eta\gamma}}{D_\rho^*(\tilde{m}_\rho)} \right\}.\end{aligned}\quad (61)$$

The δ is additional relative phase between M_{sig} and M_B , does not mentioned in Eqs. (53) and (54). It is assumed to be constant and takes into account, for example, $\rho\pi$ rescattering effects, see [41].

In the $\phi \rightarrow K^+ K^- \rightarrow a_0 \gamma$ loop model $g(m)$ has the following forms:
for $m < 2m_{K^+}$

$$\begin{aligned}g(m) &= \frac{e}{2(2\pi)^2} g_{\phi K^+ K^-} \left\{ 1 + \frac{1 - \rho_{K^+ K^-}^2(m^2)}{\rho_{K^+ K^-}^2(m_\phi^2) - \rho_{K^+ K^-}^2(m^2)} \times \right. \\ &\left[2|\rho_{K^+ K^-}(m^2)| \arctan \frac{1}{|\rho_{K^+ K^-}(m^2)|} - \rho_{K^+ K^-}(m_\phi^2) \lambda(m_\phi^2) + i\pi \rho_{K^+ K^-}(m_\phi^2) - \right. \\ &\left. - (1 - \rho_{K^+ K^-}^2(m_\phi^2)) \left(\frac{1}{4} (\pi + i\lambda(m_\phi^2))^2 - \right. \right. \\ &\left. \left. - \left(\arctan \frac{1}{|\rho_{K^+ K^-}(m^2)|} \right)^2 \right) \right] \right\},\end{aligned}\quad (62)$$

where

$$\lambda(m^2) = \ln \frac{1 + \rho_{K^+ K^-}(m^2)}{1 - \rho_{K^+ K^-}(m^2)}; \quad \frac{e^2}{4\pi} = \alpha = \frac{1}{137}. \quad (63)$$

For $m \geq 2m_{K^+}$

$$g(m) = \frac{e}{2(2\pi)^2} g_{\phi K^+ K^-} \left\{ 1 + \frac{1 - \rho_{K^+ K^-}^2(m^2)}{\rho_{K^+ K^-}^2(m_\phi^2) - \rho_{K^+ K^-}^2(m^2)} \times \right.$$

$$\times \left[\rho_{K^+K^-}(m^2)(\lambda(m^2) - i\pi) - \rho_{K^+K^-}(m_\phi^2)(\lambda(m_\phi^2) - i\pi) - \frac{1}{4}(1 - \rho_{K^+K^-}^2(m_\phi^2)) \left((\pi + i\lambda(m_\phi^2))^2 - (\pi + i\lambda(m^2))^2 \right) \right] \Bigg\}. \quad (64)$$

Note that $g(m) \rightarrow -\tilde{I}_{K^+K^-}^{K^+}(s, Q)/16\pi e$, see Eq. (16), for $m^2 \rightarrow s$, $m_\phi^2 \rightarrow -Q^2$.

The inverse propagator of the ρ meson has the following expression

$$D_\rho(m) = m_\rho^2 - m^2 - im^2 \frac{g_{\rho\pi\pi}^2}{48\pi} \left(1 - \frac{4m_\pi^2}{m^2} \right)^{3/2}. \quad (65)$$

We use coupling constants $g_{\phi K^+K^-} = 4.47$, $g_{\phi\rho\pi} = 0.803 \text{ GeV}^{-1}$ and $g_{\rho\eta\gamma} = 0.50 \text{ GeV}^{-1}$, obtained with the help of Ref. [1] data.

IX. APPENDIX III: ADDITIONAL TERMS IN χ^2 FUNCTION

The function to minimize, χ^2 function, in the present paper consists of three terms:

$$\chi^2 = \chi_{\gamma\gamma}^2 + \chi_{spec}^2 + \chi_{add}^2. \quad (66)$$

The $\chi_{\gamma\gamma}^2$ and χ_{spec}^2 are usual χ^2 functions for the $\sigma(\gamma\gamma \rightarrow \eta\pi^0, s)$ and $\eta\pi^0$ spectrum of the $\phi \rightarrow \eta\pi^0\gamma$ reaction.

The χ_{add}^2 represents additional terms to reach some restrictions: lower $f_{K\bar{K}}$ to reduce influence of the analytical continuation of the $e^{i\delta_{K\bar{K}}^{bg}}$ under the $K\bar{K}$ threshold on the $|M_{sig}|$, see Eq. (53); coupling constants close to the relations Eq. (40); not large $g_{a_0\gamma\gamma}^{(0)}$ and not very large $f_{\pi\eta'}$. The χ_{add}^2 was used to obtain Fits 1, 3, and 4. Fit 2 without χ_{add}^2 shows that the a_0 parameters not go far from the Fit 1 results.

-
- [1] K.A. Olive *et al.* (Particle Data Group), Chin. Phys. C **38**, 090001 (2014).
 - [2] F.E. Close, N. Isgur, and S. Kumano, Nucl. Phys. **B389**, 513 (1993).
 - [3] N.A. Törnqvist, Z. Phys. C **68**, 647 (1995).
 - [4] M. Albaladejo and J. A. Oller, Phys. Rev. D **86**, 034003 (2012).
 - [5] B. Kerbikov, Phys. Lett. B **596**, 200 (2004).
 - [6] J. L. Rosner, J. Phys. G **34**, S127 (2007).
 - [7] E. Klempt and A. Zaitsev, Phys. Rept. **454**, 1 (2007).

- [8] M.K. Volkov and A.E. Radzhabov, Usp. Fiz. Nauk **176**, 569 (2006) [Physics-Uspekhi **49**, 551 (2006)];
- [9] M. Harada, H. Hoshino, and Y. L. Ma, Phys. Rev. D **85**, 114027 (2012).
- [10] R. L. Jaffe, Phys. Rev. D **15**, 267 (1977); Phys. Rev. D **15**, 281 (1977); Phys. Rept. **409**, 1 (2005).
- [11] A. H. Fariborz, R. Jora, J. Schechter, and M. N. Shahid, Phys. Rev. D **84**, 094024, 113004 (2011).
- [12] L.-Y. Dai, M. R. Pennington, Phys. Rev. D **90**, 036004 (2014).
- [13] N. N. Achasov, S. A. Devyanin and G. N. Shestakov, Phys. Lett. B **108**, 134 (1982); Z. Phys. C **16**, 55 (1982).
- [14] N. N. Achasov and G. N. Shestakov, Z. Phys. C **41**, 309 (1988).
- [15] N. N. Achasov and V. N. Ivanchenko, Nucl. Phys. B **315**, 465 (1989).
- [16] N. N. Achasov and V. V. Gubin, Phys. Rev. D **56**, 4084 (1997).
- [17] M. N. Achasov *et al.* (SND Collab.), Phys. Lett. B **438**, 441 (1998); M. N. Achasov *et al.*, Phys. Lett. B **479**, 53 (2000).
- [18] M. N. Achasov *et al.* (SND Collab.), Phys. Lett. B **440**, 442 (1998); M. N. Achasov *et al.*, Phys. Lett. B **485**, 349 (2000); R. R. Akhmetshin *et al.* (CMD-2 Collab.), Phys. Lett. B **462**, 380 (1999); A. Aloisio *et al.* (KLOE Collab.), Phys. Lett. B **537**, 21 (2002).
- [19] N. N. Achasov and V.V. Gubin, Phys. Rev. D **63**, 094007 (2001).
- [20] A. Aloisio *et al.* (KLOE Collab.), Phys. Lett. B **536**, 209 (2002).
- [21] N. N. Achasov and A.V. Kiselev, Phys. Rev. D **68**, 014006 (2003).
- [22] N. N. Achasov, Nucl. Phys. A **728**, 425 (2003).
- [23] N. N. Achasov and G. N. Shestakov, Phys. Rev. D **77**, 074020 (2008).
- [24] N. N. Achasov and G. N. Shestakov, Phys. Rev. D **81**, 094029 (2010).
- [25] N.N. Achasov and G.N. Shestakov, Usp. Fiz. Nauk **54**, 799 (2011) [Physics-Uspekhi **181**, 827 (2011)].
- [26] The prediction $\Gamma(f_0(980) \rightarrow \gamma\gamma) \approx \Gamma(a_0(980) \rightarrow \gamma\gamma) \approx 0.27$ keV was done in 1982 in the frame of the four-quark MIT bag model. The Particle Data Group survey of 2014 [1] gives the following data: $\Gamma(f_0(980) \rightarrow \gamma\gamma) \approx 0.29$ keV and $\Gamma(a_0(980) \rightarrow \gamma\gamma) \approx 0.3$ keV, which is an order of magnitude smaller than the $\gamma\gamma$ width of the tensor $q\bar{q}$ resonance $\Gamma(f_2(1270) \rightarrow \gamma\gamma) \approx 3$ keV. The prediction of the ideal $q\bar{q}$ model $\Gamma(f_0(980) \rightarrow \gamma\gamma)/\Gamma(a_0(980) \rightarrow \gamma\gamma) = 25/9$ is

excluded experimentally.

- [27] N.N. Achasov, A.I. Goncharenko, A.V. Kiselev, and E.V. Rogozina, Phys. Rev. D **88**, 114001 (2013); Erratum-ibid. D **89**, 059906 (2014).
- [28] S. Uehara *et al.* (Belle Collaboration) Phys. Rev. D **80**, 032001 (2009).
- [29] The following typos are noticed in Refs. [24, 25]:
 1. The curve on Fig. 19b in Ref. [25] is drawn with $g_{\sigma\gamma\gamma}^{(0)} = 0.536 \times 10^{-3} \text{ GeV}^{-1}$ and $g_{f_0\gamma\gamma}^{(0)} = 0.652 \times 10^{-3} \text{ GeV}^{-1}$ (the multiplier 10^{-3} was missed in the text).
 2. In Table I of Ref. [24] and Appendix II of Ref. [25] $(g_{a_0\gamma\gamma}^{(0)}; g_{a'_0\gamma\gamma}^{(0)}) = (1.83; -5.9) \times 10^{-3} \text{ GeV}^{-1}$ instead of $(1.77; -11.5) \times 10^{-3} \text{ GeV}^{-1}$.
 3. The c_0 in Ref. [25] is -0.603 , not -0603 .
- [30] $g_{\rho\pi^0\gamma}g_{\rho\eta\gamma} = g_{\omega\pi^0\gamma}g_{\omega\eta\gamma}$, $m_\rho \approx m_\omega$.
- [31] N.N. Achasov and V.A. Karnakov, Z. Phys. C **30**, 141 (1986).
- [32] J.M. Blatt and V.F. Weisskopf, Theoretical Nuclear Physics (Wiley, New York, 1952), pp. 359-365 and 386-389.
- [33] One can see from Table I that the a'_0 parameters are not determined well on the present stage. The nature of this particle currently can not be fixed. For example, it is possible that a'_0 is a complex of several scalars, effectively taken into account. The question of the a'_0 parameters and nature is not important for the aims of the present work.
- [34] N.N. Achasov, Phys. Lett. B **222**, 139 (1989). It results from Eq. (7) of this paper, as for the last line of Eq. (12), it has a typo.
- [35] V.L. Chernyak and A.R. Zhitnitsky, Phys. Rep. **112**, 173 (1984).
- [36] V.N. Baier and A.G. Grozin, Fiz. Elem. Chast. At. Yad. **16**, 5 (1985) [Sov. J. Part. Nucl. **16**, 1 (1985)].
- [37] N.N. Achasov and A.A. Kozhevnikov, Phys. Rev. **D57**, 4334 (1998).
- [38] M. Masuda *et al.* (Belle Collaboration), Phys. Rev. **D93**, 032003 (2016), arXiv:1508.06757.
- [39] S. Uehara *et al.* (Belle Collaboration), Phys. Rev. D **78**, 052004 (2008).
- [40] N.N. Achasov, A.V. Kiselev and G.N. Shestakov, Pis'ma Zh. Eksp. Teor. Fiz. 102 (2015) 655 [JETP Lett. 102 (2015) 571], arXiv:1509.09150.
- [41] N.N. Achasov and A.A. Kozhevnikov, Phys. Rev. **D61**, 054005 (2000).